

Finite element analysis of maxillary incisor displacement during *en-masse* retraction according to orthodontic mini-implant position

Jae-Won Song^a
Joong-Ki Lim^b
Kee-Joon Lee^c
Sang-Jin Sung^d
Youn-Sic Chun^e
Sung-Seo Mo^f

^aDepartment of Orthodontics, Graduate School of Clinical Dental Science, The Catholic University of Korea, Seoul, Korea

^bPrivate Practice, Seoul, Korea

^cDepartment of Orthodontics, College of Dentistry, Yonsei University, Seoul, Korea

^dDivision of Orthodontics, Department of Dentistry, Asan Medical Center, Seoul, Korea

^eDepartment of Orthodontics, Ewha Womans University Mokdong Hospital, Seoul, Korea

^fDivision of Orthodontics, Department of Dentistry, St. Paul's Hospital, College of Medicine, The Catholic University of Korea, Seoul, Korea

Objective: Orthodontic mini-implants (OMI) generate various horizontal and vertical force vectors and moments according to their insertion positions. This study aimed to help select ideal biomechanics during maxillary incisor retraction by varying the length in the anterior retraction hook (ARH) and OMI position.

Methods: Two extraction models were constructed to analyze the three-dimensional finite element: a first premolar extraction model (Model 1, M1) and a residual 1-mm space post-extraction model (Model 2, M2). The OMI position was set at a height of 8 mm from the arch wire between the second maxillary premolar and the first molar (low OMI traction) or at a 12-mm height in the mesial second maxillary premolar (high OMI traction). Retraction force vectors of 200 g from the ARH (-1, +1, +3, and +6 mm) at low or high OMI traction were resolved into X-, Y-, and Z-axis components. **Results:** In M1 (low and high OMI traction) and M2 (low OMI traction), the maxillary incisor tip was extruded, but the apex was intruded, and the occlusal plane was rotated clockwise. Significant intrusion and counter-clockwise rotation in the occlusal plane were observed under high OMI traction and -1 mm ARH in M2. **Conclusions:** This study observed orthodontic tooth movement according to the OMI position and ARH height, and M2 under high OMI traction with short ARH showed retraction with maxillary incisor intrusion.

[Korean J Orthod 2016;46(4):242-252]

Key words: Finite element model, Tooth movement, Mini-implant

Received June 16, 2015; Revised December 22, 2015; Accepted January 8, 2016.

Corresponding author: Sung-Seo Mo.

Professor, Division of Orthodontics, Department of Dentistry, St. Paul's Hospital, College of Medicine, The Catholic University of Korea, 180 Wangsan-ro, Dongdaemun-gu, Seoul 02559, Korea.

Tel +82-2-958-2418 e-mail dmoos1@hanmail.net

The authors report no commercial, proprietary, or financial interest in the products or companies described in this article.

© 2016 The Korean Association of Orthodontists.

This is an Open Access article distributed under the terms of the Creative Commons Attribution Non-Commercial License (<http://creativecommons.org/licenses/by-nc/4.0>) which permits unrestricted non-commercial use, distribution, and reproduction in any medium, provided the original work is properly cited.

INTRODUCTION

En-masse retraction is beneficial because it does not require complicated techniques such as wire bending, but it provides little room for the orthodontist to adjust, except for the length of the anterior retraction hook (ARH), thereby making it difficult to obtain various tooth movement patterns. Conventional *en-masse* retraction is known to produce extrusion of upper incisor and thus difficult to apply to patients with vertical dento-alveolar excess (VDE) or gummy smile.¹⁻³

However, in recent studies about *en-masse* retraction using orthodontic mini-implants (OMI) as anchorage, Upadhyay et al.^{4,5} reported that for the orthodontic treatment of bi-alveolar protrusion patients, OMI were significantly effective for *en-masse* retraction of the maxillary incisors by promoting intrusion in the maxillary incisors and molars to reduce vertical dimension while also rotating the mandible counter-clockwise. Lim⁶ stated that in patients with a gummy smile, OMI insertion in an area with a potentially similar line of action to that of the high pull J hook Headgear could cause maxillary incisor intrusion without requiring assistance from the patient, effectively treating VDE of maxillary incisors, and Lee et al.⁷ reported that the vertical position of the incisor changed according to OMI insertion positions.

In the orthodontic field, OMI not only strengthens the anchorage but can also allow application of forces in multiple directions according to the position of insertion.^{8,9} Insertion of OMI can generate horizontal and vertical force vectors in a desired direction along with moment, resulting in effective tooth movement without a loss in anchorage.¹⁰

Although various orthodontic tooth movements can be achieved by using OMI, there is a lack of studies on this aspect. OMI insertion position was level with ARH height in a previous study about *en-masse* retraction using finite element analysis (FEA)¹¹ and a clinical study by Sia et al.,¹² but these studies did not present the various tooth movement patterns caused by height differences between OMI insertion and ARH because the retraction force was parallel with the arch wire and the vertical force was not considered. In addition, these studies put emphasis on initial angulation changes of maxillary incisor because of the arch wire bowing effect rather than tooth movement by bone remodeling, and could not account for the vertical and horizontal tooth displacement pattern. Kojima and Fukui¹³ suggested the use of a stiffer arch wire in non-extraction model to prevent overestimation of the arch wire bowing effect and obtain outcomes similar to those obtained under clinical conditions.

The purpose of this study was to identify how a

change in the force system affects tooth displacement and the occlusal plane as well as tooth angulation based on OMI insertion position and height, ARH height, and both horizontal and vertical forces associated with changes in the tooth extraction space by using FEA in an extraction model.

MATERIALS AND METHODS

Creation of the finite element model

The dental model (Model-i21D-400G; Nissin Dental Products, Kyoto, Japan) was based on adult subjects with a normal occlusion. The right maxillary teeth were scanned and outlined using a three-dimensional (3D) laser, with the first model showing an extracted first premolar (Model 1, M1) and the second model showing a 1-mm extraction space (Model 2, M2) in which initial tooth angulation was maintained and the arch form was made by reference to the extracted model by Chong et al.¹⁴ The dental arch was arranged on the basis of the broad arch form of Ormco (Orange, CA, USA).

The teeth, bracket, periodontal ligament, and alveolar bone comprised a 4-node tetrahedron. The teeth and bracket were connected without interference, and each tooth was independent and connected to the other by contact points.¹⁵ Teeth inclination and angulation were arranged as described by Germane et al.¹⁶ and Andrews.¹⁷ A curve of spee and Wilson's curve were not made. A mesio-distal sized Micro-arch[®] (Tomy Co., Tokyo, Japan) bracket was applied to the models. The bracket was attached to each tooth by placing its slots onto the facial axis point of the crown.¹⁷ The periodontal membrane thickness was consistently set at 0.2 mm as described by Coolidge.¹⁸ No alveolar bone loss was assumed. The 3D finite element model (FEM) comprised the maxillary teeth, periodontal membrane, and alveolar bone along the cemento-enamel junction (CEJ) line from the 1-mm upper height of the CEJ in a bilaterally symmetric shape (Figure 1).

The teeth, bracket, periodontal ligament, alveolar bone, and arch wire used in the model were assumed to have isotropic and homogenous linear elasticity. The Young's modulus and Poisson's ratio in the periodontal ligament and alveolar bone were set as described by Tanne et al.¹⁹ and Sung et al.²⁰ The teeth, bracket, and arch wire were assigned a Young's modulus 1,000 times larger than those used in previous studies (Table 1). Arch wire was produced separately with beam elements using stainless steel with a thickness of 0.019 × 0.025 inches. Only sliding without friction and clearance was allowed between the arch wire and bracket slot to prevent unnecessary wire-bracket play.

In M1 and M2, OMI were placed between the second maxillary premolar and the first molar at 8 mm in height

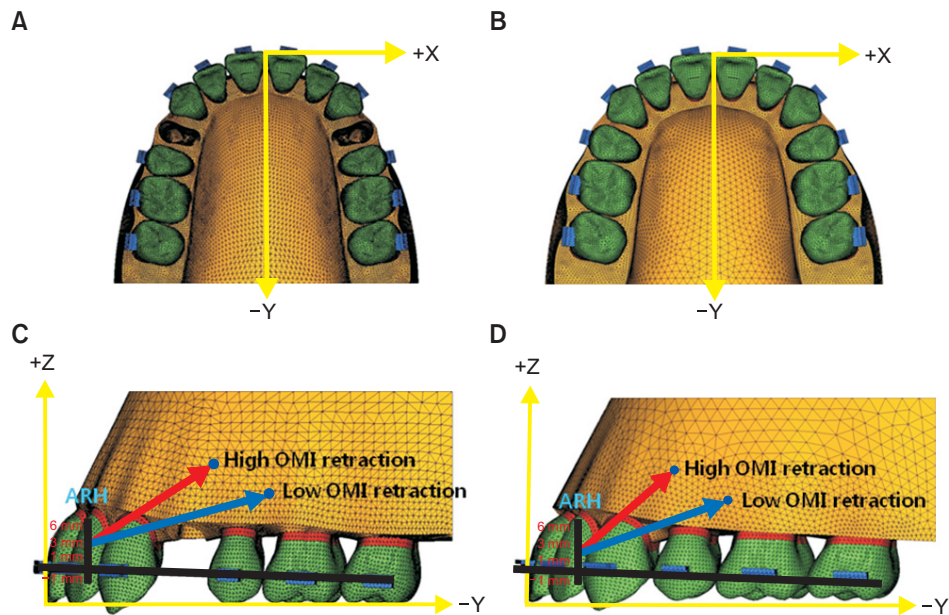


Figure 1. Three-dimensional finite element models. **A**, Occlusal view of the model with extraction of the first premolar (Model 1, M1). **B**, Occlusal view of the model with residual extraction space of 1 mm (Model 2, M2). **C**, Lateral view of the model with extraction of the first premolar (M1). **D**, Lateral view of the model with residual extraction space of 1 mm (M2).

ARH, Anterior retraction hook; OMI, orthodontic mini-implants; X, medio-lateral; +, lateral; -, medial direction; Y, antero-posterior; +, anterior; -, posterior direction; Z, superio-inferior; +, superior; -, inferior direction.

Table 1. Mechanical properties of each material

	Young's modulus (MPa)	Poisson's ratio
Teeth	2.0E + 07	0.3
Bracket	2.0E + 08	0.3
Periodontal ligament	5.0E - 02	0.49
Alveolar bone	2.0E + 03	0.3
Stainless steel wire	2.0E + 08	0.3

from the main arch wire towards the root apex area (low OMI traction) or at 12 mm from the mesial second maxillary premolar (high OMI traction).

For the ARH made of stainless steel wire of 0.8 mm diameter, +3 mm and +6 mm ARH, representing short and long crimpable hooks, respectively, were used in low OMI traction and +3 mm, +1 mm, and -1 mm, representing short crimpable hooks, soldered hooks, and reverse solder hooks, respectively, were used in high OMI retraction. The high OMI retraction model was used to magnify the vertical vector so that the long crimpable hook (+6 mm ARH) was excluded. A 200-g retraction force was added to each side of the ARH in both low and high OMI traction.

Interpretation of finite element analysis

An HP XW6400 workstation (Hewlett-Packard Co., Palo Alto, CA, USA) and general-purpose finite element program, ANSYS 11 (Swanson Analysis System, Canonsburg, PA, USA) were used to prepare the finite element.

For the baseline coordination system, the starting point was designated at the central point of the line connecting the incisal edges of the maxillary central incisors, and lateral tooth displacement in the medio-lateral direction formed the X-axis. Anterior and posterior displacement along the labio-lingual side formed the Y-axis. The superior-inferior direction formed the Z-axis, and vertical displacement was measured. The left central incisor side of the X-axis, the labial side of the Y-axis, and the root apex side of the Z-axis were designated as positive, and the occlusal plane was designated as the XY-plane (Figure 1).

The resulting tooth movement immediately after maxillary first tooth extraction as the extraction space decreased in size was compared between M1 and M2. The tooth axis change and occlusal plane rotation were also examined according to the ARH height and OMI insertion position. The central and lateral incisors were compared based on the central point of the incisal edge and root apex; the canine teeth based on the cusp tip and root apex; and the maxillary first molar based

Table 2. Amount of tooth displacement of maxillary incisors and maxillary first molar according to orthodontic mini-implant position and length of anterior retraction hook in both models with extraction of the first premolar (Model 1)

Model 1		Low OMI traction			High OMI traction		
Tooth	Reference point	Hook height (mm)	Δy (mm)	Δz (mm)	Hook height (mm)	Δy (mm)	Δz (mm)
CI	Root apex	+3	1.84E - 03	5.87E - 02	-1	-9.27E - 03	3.71E - 02
	Incisal edge		-1.20E - 01	-3.10E - 02		-6.48E - 02	-3.92E - 03
	Root apex	+6	3.15E - 03	6.10E - 02	+1	-8.10E - 03	4.07E - 02
	Incisal edge		-1.25E - 01	-3.41E - 02		-7.32E - 02	-7.42E - 03
	Root apex				+3	-6.73E - 03	4.44E - 02
	Incisal edge					-8.20E - 02	-1.12E - 02
LI	Root apex	+3	1.41E - 02	4.26E - 02	-1	-1.27E - 03	2.98E - 02
	Incisal edge		-9.29E - 02	-2.74E - 02		-5.00E - 02	-2.41E - 03
	Root apex	+6	1.59E - 02	4.38E - 02	+1	6.43E - 04	3.21E - 02
	Incisal edge		-9.72E - 02	-3.04E - 02		-5.65E - 02	-5.69E - 03
	Root apex				+3	2.76E - 03	3.44E - 02
	Incisal edge					-6.33E - 02	-9.29E - 03
C	Root apex	+3	1.43E - 02	2.34E - 02	-1	1.05E - 03	1.94E - 02
	Cusp tip		-5.36E - 02	-2.68E - 02		-2.72E - 02	-2.76E - 03
	Root apex	+6	1.58E - 02	2.34E - 02	+1	2.77E - 03	2.02E - 02
	Cusp tip		-5.61E - 02	-3.01E - 02		-3.10E - 02	-6.10 - 03
	Root apex				+3	4.65E - 03	2.09E - 02
	Cusp tip					-3.50E - 02	-9.76E - 03
FM	Mesio-buccal apex	+3	4.20E - 03	-1.49E - 02	-1	6.87E - 04	-2.04E - 03
	Mesio-buccal cusp tip		-8.42E - 03	-1.48E - 02		-1.26E - 03	-1.54E - 03
	Mesio-buccal apex	+6	4.60E - 03	1.76E - 02	+1	1.15E - 03	-4.24E - 03
	Mesio-buccal cusp tip		-9.10E - 03	-1.74E - 02		-2.16E - 03	-3.71E - 03
	Mesio-buccal apex				+3	1.66E - 03	-6.65E - 03
	Mesio-buccal cusp tip					-3.14E - 03	-6.10E - 03

OMI, Orthodontic mini-implants; CI, maxillary central incisor; LI, maxillary lateral incisor; C, maxillary canine; FM, maxillary first molar; Δy , amount of tooth displacement in Y-axis; Δz , amount of tooth displacement in Z-axis.

on the mesiobuccal cusp tip and root apex, with the X-, Y-, and Z-axis coordinate values and displacements measured in each. To more easily interpret the tooth movements using FEA, the amount of displacement of the incisal edge, cusp tip, and root apex were magnified 100 times along the Y- and Z-axis (Tables 2 and 3, Figures 2–7).

Changes in position of the center of resistance (CR) of the central maxillary incisors

Changes in position of the CR of the central maxillary incisors were calculated with coordinates of the central points of maxillary incisor edge and root apex based on a review of other previous studies. Marcuschamer et al.²¹ and Brook and Holt²² reported that the crown:root ratio was 10.5:13 and Sia et al.²³ reported that the CR was

located at approximately 0.77 of the root height from the root apex. Displacement of the CR was measured by determining the difference between the initial position of the CR and a position of the displaced CR (Table 4).

RESULTS

In M1 under low and high OMI traction, the tips of the maxillary incisors and the mesiobuccal cusp of the maxillary first molar were extruded, but the extrusion magnitude decreased as the ARH length decreased. For the root apex displacement, root apexes of the maxillary incisors were intruded, while the mesiobuccal root apex of the maxillary first molar was extruded (Tables 2 and 3, Figure 3).

In M2 under high OMI traction, intrusion occurred in

Table 3. Amount of tooth displacement of maxillary incisors and maxillary first molar according to orthodontic mini-implant position and length of anterior retraction hook in both models with residual extraction space of 1 mm (Model 2)

Model 2		Low OMI traction			High OMI traction		
Tooth	Reference point	Hook height (mm)	Δy (mm)	Δz (mm)	Hook height	Δy (mm)	Δz (mm)
CI	Root apex	+3	1.63E - 03	5.12E - 02	-1	-1.66E - 02	1.80E - 02
	Incisal edge		-1.04E - 01	-2.69E - 02		-1.89E - 02	1.62E - 02
	Root apex	+6	3.71E - 03	5.45E - 02	+1	-1.53E - 02	2.20E - 02
	Incisal edge		-1.13E - 01	-3.16E - 02		-2.82E - 02	1.24E - 02
	Root apex				+3	-1.36E - 02	2.66E - 02
	Incisal edge					-3.92E - 02	7.68E - 03
LI	Root apex	+3	1.24E - 02	3.88E - 02	-1	-1.25E - 02	1.77E - 02
	Incisal edge		-8.56E - 02	-2.33E - 02		-1.48E - 02	1.55E - 02
	Root apex	+6	1.52E - 02	4.08E - 02	+1	-1.04E - 02	2.04E - 02
	Incisal edge		-9.28E - 02	-2.78E - 02		-2.24E - 02	1.21E - 02
	Root apex				+3	-7.72E - 03	2.35E - 02
	Incisal edge					-3.14E - 02	7.76E - 03
C	Root apex	+3	1.30E - 02	2.30E - 02	-1	-8.95E - 03	1.37E - 02
	Cusp tip		-5.21E - 02	-2.22E - 02		-4.78E - 03	1.35E - 02
	Root apex	+6	1.55E - 02	2.34E - 02	+1	-7.00E - 03	1.50E - 02
	Cusp tip		-5.67E - 02	-2.67E - 02		-9.61E - 03	1.01E - 02
	Root apex				+3	-4.58E - 03	1.64E - 02
	Cusp tip					-1.54E - 02	5.94E - 03
FM	Mesio-buccal apex	+3	3.94E - 03	-1.29E - 02	-1	-2.12E - 03	5.47E - 03
	Mesio-buccal cusp tip		-8.82E - 03	-1.24E - 02		4.14E - 03	6.73E - 03
	Mesio-buccal apex	+6	4.58E - 03	-1.65E - 02	+1	-1.58E - 03	3.26E - 03
	Mesio-buccal cusp tip		-9.89E - 03	-1.58E - 02		3.07E - 03	4.57E - 03
	Mesio-buccal apex				+3	-9.09E - 04	5.60E - 04
	Mesio-buccal cusp tip					1.74E - 03	1.93E - 03

OMI, Orthodontic mini-implants; CI, maxillary central incisor; LI, maxillary lateral incisor; C, maxillary canine; FM, maxillary first molar; Δy , amount of tooth displacement in Y-axis; Δz , amount of tooth displacement in Z-axis.

the maxillary anterior crowns, root apexes, each cusp, and the root apex of the maxillary first molar, regardless of the ARH height. The intrusion magnitude of the crown was largest when the -1 mm ARH was used. In M2 under low OMI traction, extrusion was observed in the maxillary anterior crown, mesiobuccal cusp, and root apex of the maxillary first molar, and intrusion occurred in the root apexes of the maxillary incisors (Tables 2 and 3, Figure 3).

DISCUSSION

In mechanical engineering, FEA is a useful tool to analyze changes in a machine by predicting the initial response with no remodeling, but there is a difference when this approach is applied to a human body. This

is because when an orthodontic force within an elastic limit is applied, the teeth, arch wire, and bracket only show an initial response according to the existing mechanical response with no change over time, but the periodontal ligament and alveolar bone are remodeled over time after the biological response and show changes in position and shape.

Sung et al.²⁴ reported that when using OMI-based sliding mechanics, *en-masse* bodily movement of incisors was made difficult by the initial tooth movement due to elastic deformation in the periodontal ligament and bending in the teeth, alveolar bone, and arch wire in the FEM, which highlighted the limitation of FEA. For this reason, they stated that orthodontic tooth movement observed clinically would differ from the initial tooth movement shown in the FEA.

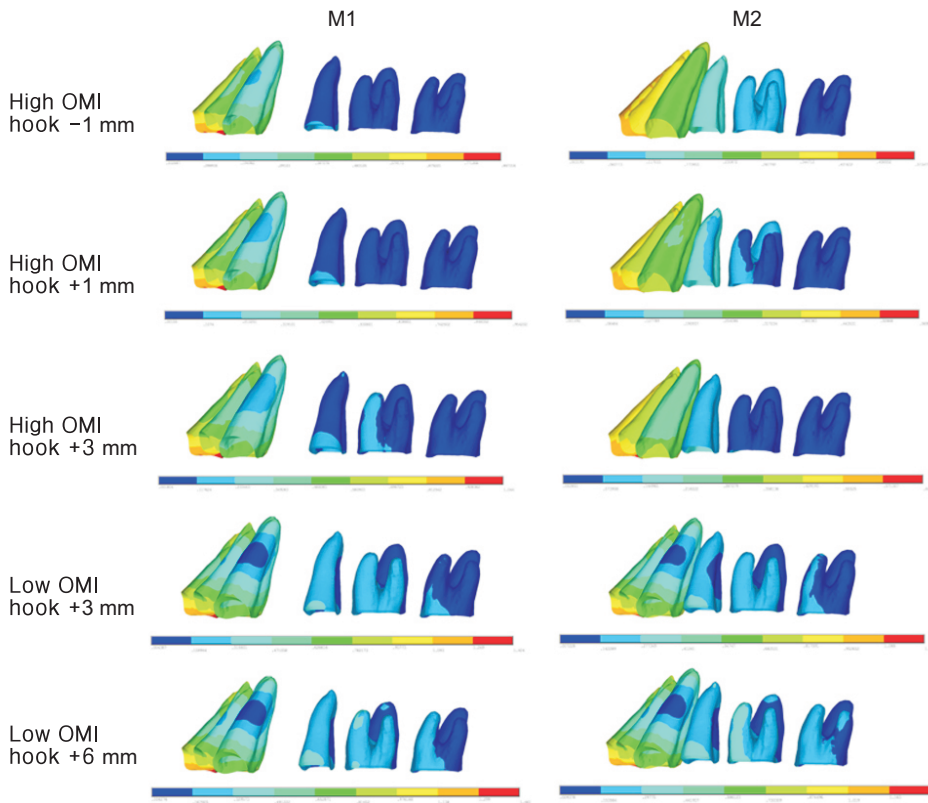


Figure 2. Von Mises stress distribution (g/mm^2). M1, Model 1; M2, Model 2; OMI, orthodontic mini-implants.

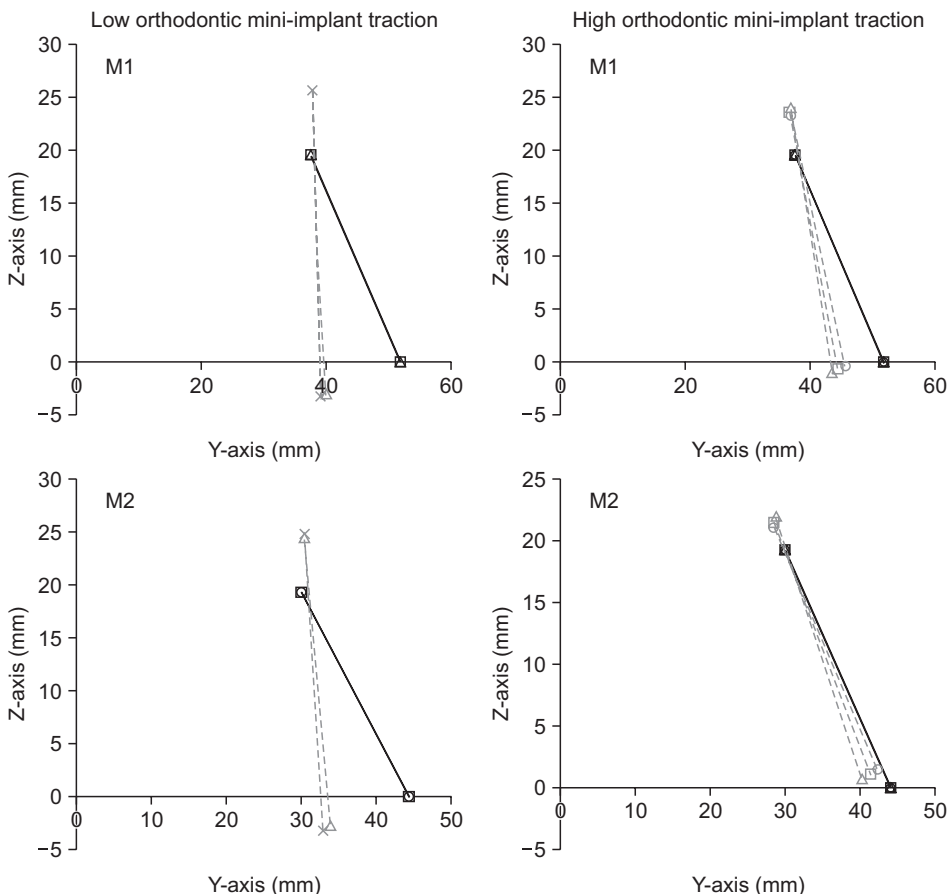


Figure 3. The axis changes of the maxillary central incisors according to the length of the anterior retraction hook under low and high orthodontic mini-implant traction in both models with extraction of the first premolar (Model 1, M1) and a residual extraction space of 1 mm (Model 2, M2). Solid line, original axis of the maxillary central incisor; dashed line, changed axis of the maxillary central incisor; ○, -1 mm hook; □, +1 mm hook; Δ, +3 mm hook; ×, +6 mm hook.

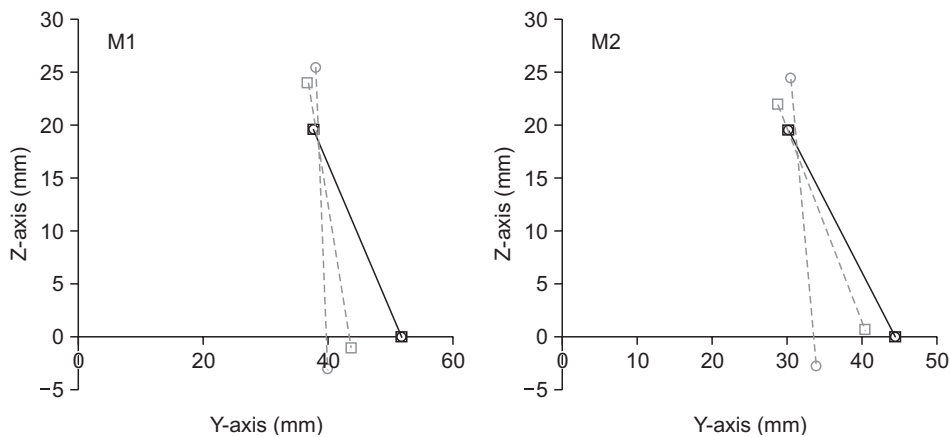


Figure 4. The axis change in the maxillary central incisor retracted by low and high orthodontic mini-implant (OMI) traction with a 3-mm anterior retraction hook in both models with extraction of the first premolar (Model 1, M1) and a residual extraction space of 1 mm (Model 2, M2). Solid line, original axis of the maxillary central incisor; dashed line, changed axis of the maxillary central incisor; ○, low OMI retraction; □, high OMI retraction.

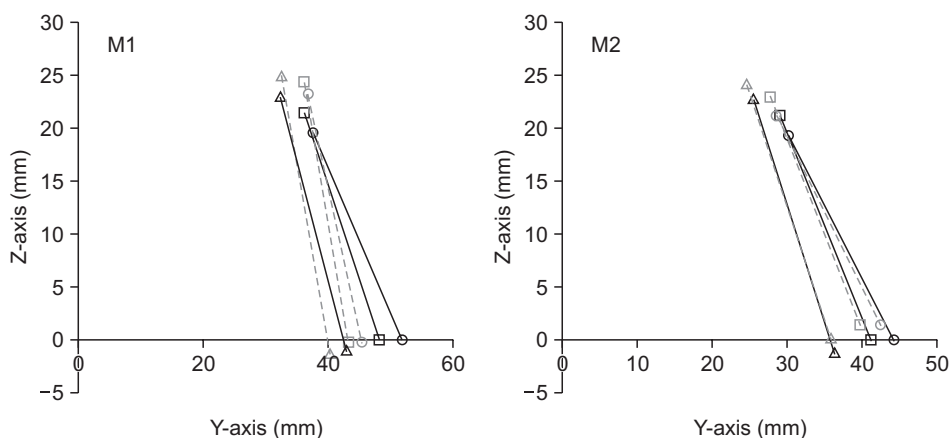


Figure 5. The axis change in the maxillary incisors retracted by high orthodontic mini-implant traction with a –1 mm anterior retraction hook in both models with extraction of the first premolar (Model 1, M1) and a residual extraction space of 1 mm (Model 2, M2). Solid line, original axis of maxillary incisors; dashed line, changed axis of maxillary incisors; ○, maxillary central incisor; □, maxillary lateral incisor; Δ, maxillary canine.

To overcome this limitation, Kojima and Fukui¹³ introduced a repeated finite element experiment method. Because tooth movement results from the periodontal ligament reaction to the external force, they assigned a typical property to the periodontal ligament, whereas the tooth, alveolar bone and arch wire were given a rigid-body property under the assumption that these three elements were not changed by external force. Under these assumptions, the experimental group with a normal property showed individual tooth movement due to arch wire bowing. During displacement, the FEA experiment was performed repeatedly to add a temporal element, and as a result, there was no signifi-

cant difference in the tooth movement between the experimental and the control groups, which showed a rigid-body property on the arch wire. They reported that this movement was similar to the orthodontic tooth movement observed clinically.

As such, although the clinically utilized arch wire is not a rigid body, the original shape seems to behave as a rigid body after long-term orthodontic treatment. In other words, because the orthodontic force imposed during orthodontic treatment is within the elasticity limit of the arch wire, if the wire is removed after orthodontic tooth movement, it maintains its initial shape without deformation. Therefore, in the finite

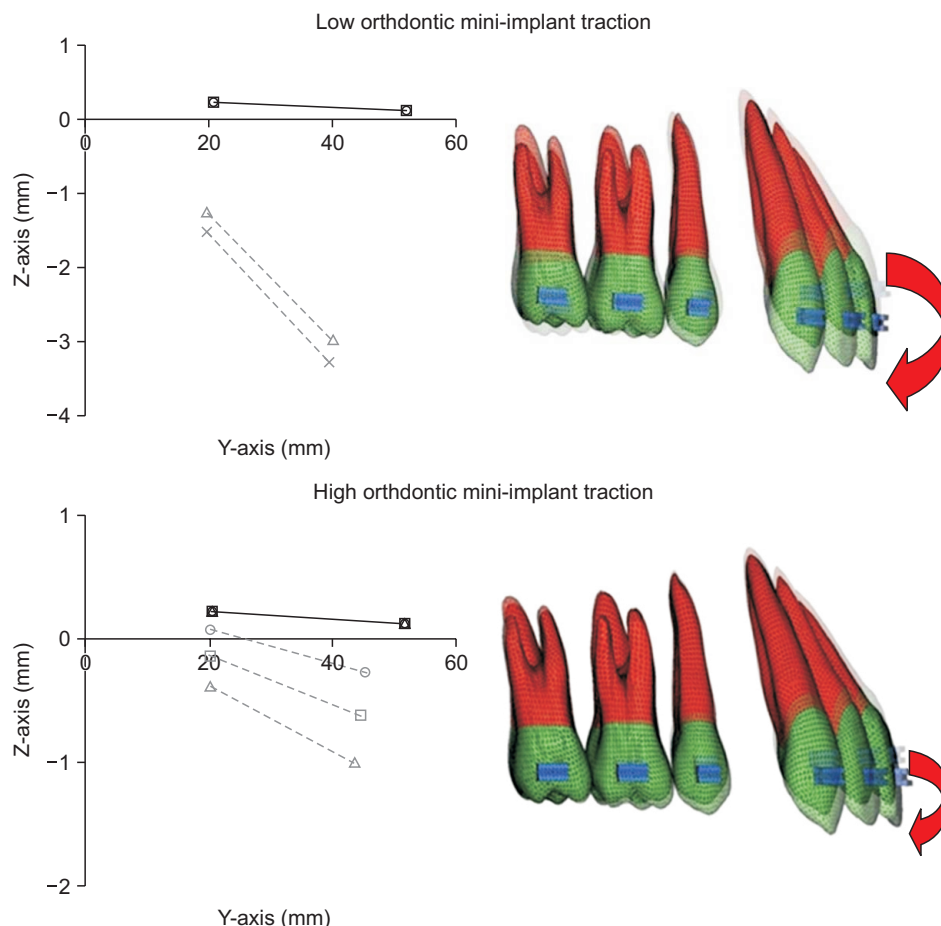


Figure 6. Movement pattern of the model with extraction of the first premolar (Model 1, M1). The rotation of the occlusal plane according to the length of anterior retraction hook used in the model with extraction of the first premolar (M1) under low and high orthodontic mini-implant traction. Solid line, original occlusal plane; dashed line, rotated occlusal plane; ○, -1 mm hook; □, +1 mm hook; △, +3 mm hook; ×, +6 mm hook.

element experiment, considering the tooth movement caused by biologic factors such as periodontal ligament and alveolar bone remodeling, it seemed valid to assume no deformation in the tooth and bracket by the external force and to increase the arch wire property in order to avoid arch wire bowing. For this reason, the present study designated a 1,000-times stronger property to the teeth, bracket, and arch wire in the FEM (Table 1).

Unlike in a previous study¹¹ that investigated tooth movement according to OMI insertion height and ARH height, in this finite element study, the models for low and high OMI traction in *en-masse* retraction were analyzed immediately after extraction and once the extraction space narrowed to 1 mm to determine the changes in the force system caused by extraction space changes.

M1 and M2 under low and high OMI traction both generated a retraction force toward the posterior and superior, and theoretically, the maxillary incisors should have shown intrusion movement (+Z direction). However, we found that only in M2 (high OMI traction), the incisor edges of the maxillary incisors were intruded. In M1 (low and high OMI traction) and M2 (low OMI traction), the incisor edges of the maxillary incisors were extruded (Tables 2 and 3, Figure 3). This analysis

result was consistent, to some extent, with a finding by Lee et al.,⁷ which reported that OMI inserted into the mesial second premolar area for incisor retraction resulted in greater intrusion of all of the incisor tips and root apices; however, when the OMI were inserted in the typical position between the second premolar and first molar, intrusion only occurred at the root apices of the incisors. As a result, the incisor edges of the maxillary incisors were extruded but the root apices were intruded, creating difficulty in interpreting tooth movement.

Therefore, to analyze the tooth movement, the displacement in CR of the maxillary central incisors must be used. The present study sought to identify the vertical and horizontal movement of the CR in order to assess maxillary incisor intrusion. We found that even when the maxillary central incisal edges were extruded and root apices were intruded, all the vertical CR positions showed intrusion despite the existence of tipping movement (Table 4). These findings are consistent with those obtained by van Steenberg et al.²⁵ and Choy et al.,²⁶ who found that significant root apex intrusion indicated intrusion of the CR.

In the present study, movement in the maxillary

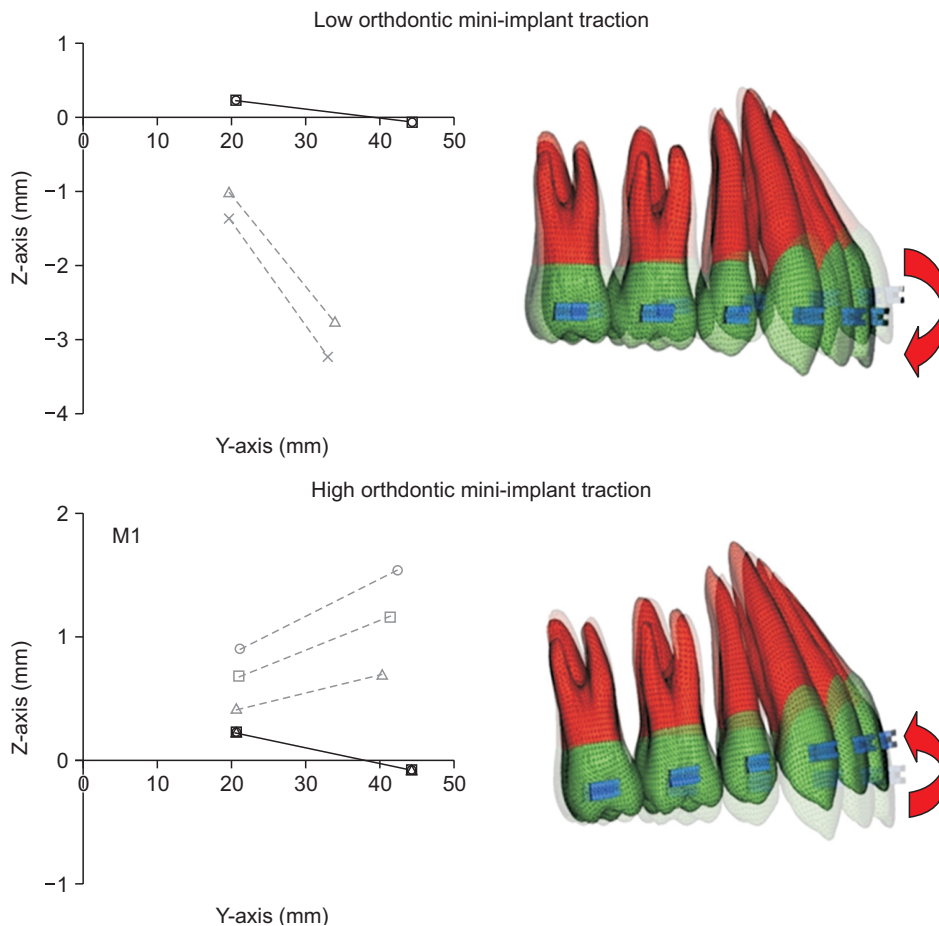


Figure 7. Movement pattern of the model with residual extraction space of 1 mm (Model 2, M2). The rotation of the occlusal plane according to the length of the anterior retraction hook used in the model with residual extraction space of 1 mm (M2) under low and high orthodontic mini-implant traction. Solid line, original occlusal plane; dashed line, rotated occlusal plane; ○, -1 mm hook; □, +1 mm hook; △, +3 mm hook; ×, +6 mm hook.

Table 4. Displacement of the center of resistance in maxillary central incisors

OMI traction with change of hook length	Model 1		Model 2	
	U CR y (mm)	U CR z (mm)	U CR y (mm)	U CR z (mm)
High OMI traction -1 mm hook	-3.291E-02	1.966E-02	-1.758E-02	1.724E-02
High OMI traction +1 mm hook	-3.582E-02	2.023E-02	-2.080E-02	1.790E-02
High OMI traction +3 mm hook	-3.879E-02	2.072E-02	-2.451E-02	1.854E-02
Low OMI traction +3 mm hook	-4.985E-02	2.051E-02	-4.339E-02	1.793E-02
Low OMI traction +6 mm hook	-5.158E-02	2.049E-02	-4.592E-02	1.782E-02

OMI, Orthodontic mini-implants; U CR y, displacement amount of center of resistance in Y-axis; U CR z, displacement amount of Center of resistance in Z-axis.

incisor was compared under low and high OMI traction conditions. Under low OMI traction, both M1 and M2 showed tipping movement and crown extrusion, and there was no significant difference. Under high OMI traction, M1 showed tipping movement and crown extrusion, but M2 showed movement similar to the bodily tooth movement and crown intrusion. We also observed that the shorter the ARH height (negative value), the better the crown torque was maintained (Figure 3).

This finding indicated that even though identical biomechanics was utilized during the initial treatment stage, as the extraction spaces closed during treatment, the system of forces also changed. In addition, despite the same ideal biomechanics, extrusion and intrusion of the incisor tips changed as the extraction space closed. Therefore, depending on the time point during treatment, it may be difficult to identify incisor extrusion or intrusion. In this regard, Upadhyay et al.⁵ and Park et al.²⁷ stated that even after complete closure of

the extraction space, if the retraction force continued for several months, then the intrusion force could affect the entire maxillary arch and cause intrusion of the maxillary molars. When comparing low and high OMI traction with a 3-mm ARH, a greater decrease in the lingual tipping movement of the maxillary central incisor and a greater increase in the crown intrusion were observed and the incisor torque was maintained well in high OMI traction than observed in low OMI traction (Figure 4).

A combination of -1 mm ARH and high OMI traction during *en-masse* retraction of the maxillary incisors generated the most favorable intrusion along the tooth longitudinal axis among all the ARH height and OMI position combinations. The lingual tipping movement of the maxillary incisors in M2 decreased compared to that in M1, showing a pattern of intrusion closest to the bodily tooth movement (Figure 5).

Lim⁶ recommended that in order to improve the vertical force vector, OMI should be inserted between the first and second premolars, and at the muco-gingival junction area while turning ARH towards the occlusal side. Moreover, as the extraction spaces grow narrower, the geometry changes and retracts the incisors; thus, the horizontal force vector mostly decreases, while the vertical force vector increases. In this manner, maxillary incisor intrusion force increased whereas the retraction force decreased, expanding the labial flaring moment of the crown. This is similar to the findings in the present study that low OMI traction, which is primarily used clinically, showed extrusion of the incisor tip regardless of changes in the extraction space size, whereas high OMI traction resulted in extrusion of the incisor tip early during treatment but transitioned to show intrusion of the incisor tip as the extraction space closed.

During *en-masse* retraction, the occlusal plane, the line connecting the incisal edge of the central point of the maxillary central incisor and the mesio-buccal cusp tip of the first molar, which was presumed to be the functional occlusal plane, in M1 (low and high OMI traction) and M2 (low OMI traction) showed a clockwise rotation. Therefore, the apparent maxillary incisal edge extrusion and root apex intrusion may not simply indicate absolute extrusion in the maxillary incisor tip, but may also indicate the effect of occlusal plane rotation on the maxillary incisal edge. During low OMI traction, clockwise rotation was observed in the occlusal plane accompanying first molar extrusion immediately after extraction and as the extraction space closed. This was consistent with reports stating that molar extrusion occurs during retraction.²⁸ In addition, during high OMI traction, the M1 model showed clockwise rotation of the occlusal plane accompanying the maxillary incisal edge and first molar extrusion. In contrast, in M2 under high OMI retraction, counter-clockwise rotation of the

occlusal plane accompanying the maxillary incisor and first molar intrusion was observed (Figures 6 and 7). In M1, high OMI was located anterior and higher than low OMI, so high OMI retraction showed less clockwise rotation of the occlusal plane because there was a greater vertical component of the retraction force than low OMI retraction. In M2, the distance between OMI and ARH became shorter as the extraction space closed so that there was a greater vertical component compared to M1. Accordingly, low OMI retraction showed less clockwise rotation of the occlusal plane and high OMI retraction even showed counter-clockwise rotation of the occlusal plane. M1 was a transient state that continued to M2 eventually. In M2 the extraction spaces were nearly closed, which resembles the clinical state at the end of treatment. This result in M2 under high OMI was consistent with the findings obtained by Lim⁶ and Upadhyay et al.^{4,5} that high OMI traction showed the intrusion of the entire maxillary arch accompanying maxillary molar intrusion, and even caused a slight mandible autorotation.

This study had some limitations associated with the fact that the interplay between the arch wire and bracket and changes in the tooth axis inclination generated during extraction space closure were not considered in FEM, which meant that this aspect could not reflect the actual biological response within the human body to orthodontic treatment. Nevertheless, based on the present findings, high OMI traction was found to have effective ideal biomechanics, especially for gummy-smile patients with maxillary VDE.

CONCLUSION

This study observed various orthodontic tooth movements according to the OMI insertion position and height, ARH height, and tooth extraction space changes. The tooth movement changed as the extraction space closed, and M2 under high OMI traction with short ARH showed retraction with maxillary incisor intrusion.

REFERENCES

1. Cha BK, Lee JY, Jost-Brinkmann PG, Yoshida N. Analysis of tooth movement in extraction cases using three-dimensional reverse engineering technology. *Eur J Orthod* 2007;29:325-31.
2. Cho MY, Choi JH, Lee SP, Baek SH. Three-dimensional analysis of the tooth movement and arch dimension changes in Class I malocclusions treated with first premolar extractions: a guideline for virtual treatment planning. *Am J Orthod Dentofacial Orthop* 2010;138:747-57.
3. Lai EH, Yao CC, Chang JZ, Chen I, Chen YJ. Three-

- dimensional dental model analysis of treatment outcomes for protrusive maxillary dentition: comparison of headgear, miniscrew, and miniplate skeletal anchorage. *Am J Orthod Dentofacial Orthop* 2008;134:636-45.
4. Upadhyay M, Yadav S, Nagaraj K, Patil S. Treatment effects of mini-implants for en-masse retraction of anterior teeth in bialveolar dental protrusion patients: a randomized controlled trial. *Am J Orthod Dentofacial Orthop* 2008;134:18-29.e1.
 5. Upadhyay M, Yadav S, Patil S. Mini-implant anchorage for en-masse retraction of maxillary anterior teeth: a clinical cephalometric study. *Am J Orthod Dentofacial Orthop* 2008;134:803-10.
 6. Lim JK. Gummy smile correction using mini implant. *Korean J Clin Orthod* 2010;9:14-31.
 7. Lee KJ, Park YC, Hwang CJ, Kim YJ, Choi TH, Yoo HM, et al. Displacement pattern of the maxillary arch depending on miniscrew position in sliding mechanics. *Am J Orthod Dentofacial Orthop* 2011;140:224-32.
 8. Kim SJ, Chun YS, Jung SH, Park SH. Three dimensional analysis of tooth movement using different types of maxillary molar distalization appliances. *Korean J Orthod* 2008;38:376-87.
 9. Lee HA, Park YC. Treatment and posttreatment changes following intrusion of maxillary posterior teeth with miniscrew implants for open bite correction. *Korean J Orthod* 2008;38:31-40.
 10. Mo SS, Kim SH, Sung SJ, Chung KR, Chun YS, Kook YA, et al. Factors controlling anterior torque with C-implants depend on en-masse retraction without posterior appliances: biocreative therapy type II technique. *Am J Orthod Dentofacial Orthop* 2011;139:e183-91.
 11. Tominaga JY, Tanaka M, Koga Y, Gonzales C, Kobayashi M, Yoshida N. Optimal loading conditions for controlled movement of anterior teeth in sliding mechanics. *Angle Orthod* 2009;79:1102-7.
 12. Sia S, Shibazaki T, Koga Y, Yoshida N. Experimental determination of optimal force system required for control of anterior tooth movement in sliding mechanics. *Am J Orthod Dentofacial Orthop* 2009;135:36-41.
 13. Kojima Y, Fukui H. A finite element simulation of initial movement, orthodontic movement, and the centre of resistance of the maxillary teeth connected with an archwire. *Eur J Orthod* 2014;36:255-61.
 14. Chong DR, Jang YJ, Chun YS, Jung SH, Lee SK. The evaluation of rotational movements of maxillary posterior teeth using three dimensional images in cases of extraction of maxillary first premolar. *Korean J Orthod* 2005;35:451-8.
 15. Jeong GM, Sung SJ, Lee KJ, Chun YS, Mo SS. Finite-element investigation of the center of resistance of the maxillary dentition. *Korean J Orthod* 2009;39:83-94.
 16. Germane N, Bentley BE Jr, Isaacson RJ. Three biologic variables modifying faciolingual tooth angulation by straight-wire appliances. *Am J Orthod Dentofacial Orthop* 1989;96:312-9.
 17. Andrews LF. The straight-wire appliance. Explained and compared. *J Clin Orthod* 1976;10:174-95.
 18. Coolidge ED. The thickness of the human periodontal membrane. *J Am Dent Assoc Dent Cosm* 1937;24:1260-70.
 19. Tanne K, Sakuda M, Burstone CJ. Three-dimensional finite element analysis for stress in the periodontal tissue by orthodontic forces. *Am J Orthod Dentofacial Orthop* 1987;92:499-505.
 20. Sung EH, Kim SJ, Chun YS, Park YC, Yu HS, Lee KJ. Distalization pattern of whole maxillary dentition according to force application points. *Korean J Orthod* 2015;45:20-8.
 21. Marcuschamer E, Tsukiyama T, Griffin TJ, Arguello E, Gallucci GO, Magne P. Anatomical crown width/length ratios of worn and unworn maxillary teeth in Asian subjects. *Int J Periodontics Restorative Dent* 2011;31:495-503.
 22. Brook AH, Holt RD. The relationship of crown length to root length in permanent maxillary central incisors. *Proc Br Paedod Soc* 1978;8:17-20.
 23. Sia S, Koga Y, Yoshida N. Determining the center of resistance of maxillary anterior teeth subjected to retraction forces in sliding mechanics. An in vivo study. *Angle Orthod* 2007;77:999-1003.
 24. Sung SJ, Jang GW, Chun YS, Moon YS. Effective en-masse retraction design with orthodontic mini-implant anchorage: a finite element analysis. *Am J Orthod Dentofacial Orthop* 2010;137:648-57.
 25. van Steenberghe E, Burstone CJ, Prah-Andersen B, Aartman IH. The relation between the point of force application and flaring of the anterior segment. *Angle Orthod* 2005;75:730-5.
 26. Choy K, Kim KH, Burstone CJ. Initial changes of centres of rotation of the anterior segment in response to horizontal forces. *Eur J Orthod* 2006;28:471-4.
 27. Park HS, Lee SK, Kwon OW. Group distal movement of teeth using microscrew implant anchorage. *Angle Orthod* 2005;75:602-9.
 28. Park HM, Kim BH, Yang IH, Baek SH. Preliminary three-dimensional analysis of tooth movement and arch dimension change of the maxillary dentition in Class II division 1 malocclusion treated with first premolar extraction: conventional anchorage vs. mini-implant anchorage. *Korean J Orthod* 2012;42:280-90.